Electric Power Systems Research 163 (2018) 164–173

Contents lists available at ScienceDirect

Electric Power Systems Research

journal homepage: www.elsevier.com/locate/epsr

Privacy-preserving optimal scheduling of integrated microgrids

Abdullah Albaker[a], Alireza Majzoobi[a], Guoshun Zhao[b], Jie Zhang[b], Amin Khodaei[a,*]

[a] Department of Electrical and Computer Engineering, University of Denver, Denver, CO 80210, USA
[b] Department of Mechanical Engineering, University of Texas at Dallas, Richardson, TX 75080, USA

ARTICLE INFO

Keywords:
Distributed energy resources
Grid-connected operation
Integrated microgrids
Islanded operation
Privacy-preserving optimal scheduling

ABSTRACT

The increasing penetration of microgrids in distribution networks, as a viable option for end-use customers to increase load-point reliability and power quality, will result in formation of many interconnected microgrids in a not so far future. This paper considers a case in which multiple microgrids are geographically close and electrically connected, and studies anticipated interactions among these microgrids and also between the microgrids and the utility grid, during grid-connected and islanded operation modes. A model for the optimal scheduling of integrated microgrids is further proposed. The model is first developed with the objective of minimizing the aggregated operation cost and is accordingly decomposed into individual optimal scheduling problems using the Lagrangian relaxation method to take prevailing privacy issues into account. The microgrids capability in operating in the islanded mode for multiple hours is scrutinized by a T–τ islanding criterion. Numerical simulations exhibit the merits and the effectiveness of the proposed model via simulations on a system of integrated microgrids.

1. Introduction

Microgrids, as small-scale power systems integrating various types of distributed generators (DGs), controllable loads, and distributed energy storage (DES), are significantly deployed over the past few years and are anticipated to grow more in the near future. Microgrids improve the overall system security, resiliency, and load-point reliability and further address challenges related to economics and environmental concerns by enabling the utilization of emission free renewable DGs, such as solar photovoltaic (PV) and small wind turbines [1–4]. Microgrids are capable to be fully islanded from the utility grid during upstream disturbances, which is recognized as the microgrids' most significant feature. This feature enhances the load-point reliability for the local customers and provides considerable societal cost savings [5–8]. This growing penetration will result in emergence of networks of microgrids, which not only exchange power during the grid-connected mode, but could also provide support for other microgrids during the islanded mode. This integration can potentially provide considerable benefits for the system and also for individual customers, including (1) reducing the system aggregated operation cost and customer electricity payments, (2) reducing power losses at the distribution level and increasing energy efficiency, (3) reducing potential load curtailments during islanded operation, and (4) supporting renewable generation integration.

Several studies on integrated microgrids, which are also commonly called interconnected microgrids, networked microgrids, or microgrid clusters, can be found in the literature. The application of the game theory in managing the operation of integrated microgrids was discussed in Refs. [9,10]. In Ref. [11] two microgrids were integrated and tested using the HOMER software. In Ref. [12], an optimization problem was studied based on model predictive control for a network of microgrids. The study in Ref. [13] solved an off-line optimization problem and proposed a distributed algorithm for the optimal off-line energy management solution of integrated microgrids. The study in Ref. [14] proposed a method of joint optimization and distributed control of integrated microgrids. In Ref. [15] a distributed optimization method for generation scheduling of integrated microgrids using the alternating direction method of multipliers was proposed. A modeling framework for estimating the power exchange capability between the integrated microgrids and a distribution network was developed in Ref. [16]. The study in Ref. [17] proposed a technique based on recurrent neural network to achieve optimal operation of a microgrid connected to the utility grid. From the perspective of cybersecurity and resilience studies in integrated microgrids, a cyber-network communication system was proposed for multiple microgrids in Ref. [18]. In Ref. [19], the interactions between distribution network operation and integrated microgrids were characterized. In addition to cybersecurity and resilience, state estimation was implemented in integrated microgrids in Ref. [20]. A multi-microgrid state estimation and fuzzy state estimation were presented in Ref. [21], aiming to study the increase of microgeneration

* Corresponding author.
E-mail address: amin.khodaei@du.edu (A. Khodaei).

https://doi.org/10.1016/j.epsr.2018.06.007
Received 14 November 2017; Received in revised form 13 May 2018; Accepted 8 June 2018
0378-7796/ © 2018 Elsevier B.V. All rights reserved.

Nomenclature

Indices

ch	Superscript for energy storage charging mode
d	Index for loads
dch	Superscript for energy storage discharging mode
i	Index for DERs
s	Index for scenarios
t	Index for time
m,n	Index for microgrids

Sets

A	Set of all DERs
D_A	Set of adjustable loads
G	Set of dispatchable units
T_K	Set of intra-hour time periods
M	Set of microgrids
N	Set of scenarios
S	Set of energy storage systems
T_T	Set of inter-hour time periods

Parameters

c	Generation marginal cost
DR	Ramp down rate
DT	Minimum down time
E	Load total required energy
MC	Minimum charging time
MD	Minimum discharging time
MU	Minimum operating time
U	Islanding state (0 when islanded, 1 otherwise)
UR	Ramp up rate
UT	Minimum up time
γ	Step size for Lagrangian multiplier update
ρ	Market price
λ	Connected microgrid power exchange price
α, β	Specified start and end times of adjustable loads
η	Energy storage efficiency
μ	Penalty coefficient
υ	Value of lost load
Ψ	Probability of islanding scenarios

Variables

C	Energy storage available (stored) energy
D	Load demand
I	Commitment state of dispatchable units (1 when committed, 0 otherwise)
LS	Load curtailment in islanded operation
P	DER output power
P^M	Utility grid power exchange
P^G	Power exchange with the connected microgrid
SD	Shut down cost
SU	Startup cost
T^{ch}	Number of successive charging hours
T^{dch}	Number of successive discharging hours
T^{on}	Number of successive ON hours
T^{off}	Number of successive OFF hours
τ	Time period
u	Energy storage discharging state (1 when discharging, 0 otherwise)
v	Energy storage charging state (1 when charging, 0 otherwise)
z	Adjustable load state (1 when operating, 0 otherwise)

penetration in distribution network through the exploitation and extension of the microgrid technology. Control problems of integrated microgrids were studied in Refs. [22–28]. A study to assess the merits and drawbacks of the integrated microgrids using multi-criterion decision aids was presented in Ref. [22]. Advanced control functionality to manage the increased penetration of DGs, DES, and active loads under microgrid and integrated microgrids concepts were presented in Ref. [23]. The study in Ref. [24] described a method for tertiary control level for load sharing. A real-time tertiary control algorithm for DC microgrid clusters with high penetration of renewable DGs is implemented and developed in Ref. [25]. In Ref. [26], a strategy for designing a communication and control infrastructure in a distribution system based on the virtual microgrid concept was presented. In Ref. [27], a new decentralized control scheme for managing integrated microgrids through self-organization, and decentralized scheduling and dispatch was proposed. Distributed control schemes were presented and tested in [28] for integrated low-voltage DC microgrids. Research focusing on the compromise between reliability and cost in integrated microgrids was discussed in Refs. [29–32]. In Ref. [29], the concept of integrated microgrids was discussed and the question of how to dispatch the integrated microgrids in a distribution system was raised. The small signal modeling and stability issues in DC microgrids and integrated DC microgrids was addressed in Ref. [30]. Modular-architecture microgrids were discussed in Ref. [31] to assure reliability, expansibility, and controlled cost in integrated microgrids. In Ref. [32], a probabilistic Monte Carlo based iterative methodology for the optimal planning of integrated microgrids was applied to a six-microgrid system operating in the islanded mode. A promising type of integrated microgrids, called provisional microgrids, was put forward and discussed in detail in Refs. [33–35]. As provisional microgrids do not have the ability to be islanded on their own, they will transfer power from coupled microgrids in the islanded mode. Many studies were made in the literature on the optimization of integrated microgrids. In Ref. [36], an algorithm for multi-objective optimal power flow was used, and decentralized power dispatch model was described in Ref. [37]. The study in Ref. [38] dealt with potential benefits from individual and integrated microgrids in terms of economy, loss avoidance, and emissions reduction, using electricity market prices, with different renewable generation penetration levels. The study in Ref. [39] presented an integrated energy exchange scheduling for a multi-microgrid system under a pricing strategy using adjusted prices, and further proposed a decentralized optimal scheduling strategy for the microgrid central controller to minimize the microgrids operation cost and satisfy the consumers' needs. The study in Ref. [40] developed a joint energy trading and scheduling strategy for integrated autonomous microgrids. In addition, it designed an incentive mechanism using Nash bargaining theory and investigated the possible interaction among the integrated microgrids. An optimal economic dispatch strategy utilizing a genetic algorithm was proposed in Ref. [41] for two integrated microgrids that are connected with a single energy storage system. The objective is to minimize the operation cost and find the optimal production of the distributed generators. In Ref. [42] a distributed mechanism for energy trading between the integrated microgrids was proposed in a competitive market based on a game-theoretic analysis, where the proposed game-theoretic strategy provides incentives for energy trading between the integrated microgrids. The study in Ref. [43] proposed a stochastic and probabilistic modeling framework to minimize the operation cost of each microgrid in a multi-microgrid system, and utilized the particle

swarm optimization algorithm to solve the optimization problem. In Ref. [44] an energy management framework for the integrated microgrids was presented, where the scenario-based two-stage stochastic optimization approach was proposed to capture the uncertainties related to the load demand and the generation of renewable energy resources. The study in Ref. [45] proposed a system of systems framework for optimizing the operation of active distribution grids based on a decentralized optimization approach to maximize the benefit of each independent system. The study in Ref. [46] designed a bargaining-based energy trading market for the energy trading among the integrated microgrids and proposed a decentralized algorithm to solve the bargaining problem. The study in Ref. [47] proposed a communicative scheduling model for the integrated microgrids, where the local power exchange price and the unused capacity signals are iteratively exchanged among the integrated microgrids until the optimal schedule is found.

The prior work on integrated microgrids neglect some important practical factors such as privacy preservation, islanding, and a guarantee on solution optimality. This paper builds on existing work on integrated microgrids operation and proposes a model with following contributions:

- A privacy-preserving model for the optimal scheduling problem of integrated microgrids is proposed, to ensure least possible data sharing between the microgrids.
- The proposed model maximizes the system-level reliability while minimizing individual microgrids and system-aggregated operation cost.
- The proposed model is based on a high resolution scheduling, which takes into account intra-hour and inter-hour time periods to capture the variability and volatility of the renewable generation and loads.
- The grid-connected and the islanded operation modes of the integrated microgrids are coordinated through an iterative method which is capable of managing the intricate dependencies between these two modes.

A Lagrange Relaxation (LR) method is applied to decompose the integrated problem to a set of smaller and individual scheduling problems for each microgrid. To achieve this, the inter-microgrids power transfer is penalized with a proper penalty coefficient and the problem is decomposed accordingly [48–51]. The mutual power exchange of integrated microgrids is checked after each Lagrangian iteration until equality is obtained.

The remainder of this paper is organized as follows. Section 2 provides the model outline of integrated microgrids. Section 3 formulates the optimal scheduling problem along with the proposed decomposition strategy. Section 4 provides numerical simulations of the proposed model when applied to a test system. Discussions and conclusions are provided in Section 5.

2. Integrated microgrids framework

Each microgrid within the integrated framework has clearly defined electrical boundaries and is operated by its associated master controller, while having the capability to operate in both grid-connected and islanded modes [1–3]. If operated independently of other microgrids, each microgrid would supply local loads using local resources and power purchase from utility grid during the grid-connected mode (i.e., economic operation), while trying to minimize load curtailments once switched to the islanded mode (i.e., reliable operation) [6–8]. In integrated microgrids, however, each microgrid has an additional source to leverage during the grid-connected and islanded modes, i.e., the power exchanged with the connected microgrids. In this case, if a microgrid has any surplus generation during the grid-connected mode, it can sell this generation to connected microgrids and accordingly increase its economic benefits and reduce its operation cost. Moreover, if a microgrid has unused capacity during the islanded mode, it can provide required generation for connected microgrids [10–12,47]. This transactive strategy would enhance economic benefits for the microgrid that sells energy and improves reliability for the microgrid that purchases energy.

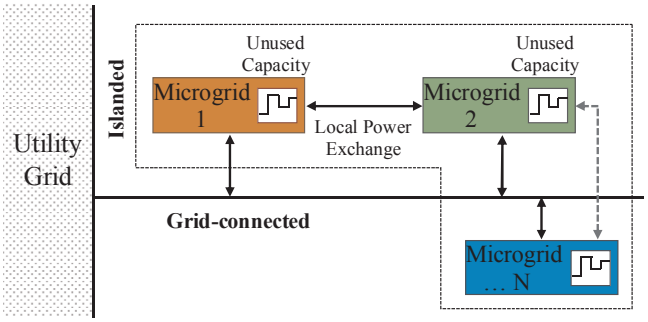

Fig. 1. Integrated microgrids are connected to the same upstream substation.

Fig. 1 depicts possible interactions of a microgrid, within the integrated microgrids framework, with the utility grid and other connected microgrids. Each microgrid has multiple options to supply local loads, e.g., from the utility grid or from other connected microgrids. Integrated microgrids operate simultaneously in the islanded mode in response to utility grid failures and/or voltage fluctuations, where it is assumed that the connection between each microgrid is maintained during islanding.

The proposed integrated microgrids framework attempts to minimize both the system aggregated operation cost (that consists of the operation cost of each individual microgrid) and the operation cost of each microgrid simultaneously. Generally, each microgrid is locally controlled by its own master controller and the system operator does not have any information on microgrids operations. In order to minimize system aggregated operation cost, the operation cost of each microgrid needs to be locally minimized while considering proper coordination between integrated microgrids. To this end, a LR method is proposed in this paper to address the multi-level coordination challenge by “relaxing” or temporarily ignoring the coupling constraints. The LR decomposition procedure generates a separable problem by integrating some coupling constraints into the objective function, through “penalty factors” which are functions of the constraint violation [49–51]. These penalty factors, referred to as Lagrangian multipliers, are determined iteratively.

In addition, a multiple time-scale operation framework is developed in this work, comprising an hourly grid-connected operation and sub-hourly islanded operations. Short-time periods are employed to more accurately capture rapid changes in load and renewable generation as well as short islanding durations [6,52]. The selection of a proper time period for scheduling represents a tradeoff between computational accuracy and efficiency. It is worth to mention that in order to characterize the microgrid islanding capability, a T–τ islanding criterion as proposed in Ref. [7] is applied, in which T and τ represent the total number of hours in scheduling horizon and the number of consecutive hours which the microgrid can operate in islanded mode, respectively. It should be mentioned that in terms of privacy, the proposed optimal scheduling model protects the microgrids’ privacy by sharing minimum possible data among microgrids, which only includes the price signal of the local power exchange.

3. Integrated microgrids problem formulation

To determine the optimal schedule of all integrated microgrids, the overall system aggregated problem (also called integrated grid problem) is first modeled, and further decomposed to obtain proper optimal scheduling problems for each individual microgrid as well as the

price signals that will be used for coordinating the power exchange among the integrated microgrids.

3.1. Integrated grid problem

The aggregated operation cost of the integrated system is minimized, which is represented by the following objective function:

$$\min \tau \sum_{m\in M}\sum_{t\in T_T}\sum_{k\in T_K}\sum_{s\in N}\psi_s\left(\sum_{i\in G} c_{mi}P_{mi,tks} + \rho_{m,tk}P^{M}_{m,tks} + \sum_{n\in M,n\neq m}\lambda_{mn,tk}P^{G}_{mn,tks} + \upsilon_{m,tk}LS_{m,tks}\right) \quad (1)$$

This objective function represents four distinct terms including the generation cost of all dispatchable DGs, the cost of power exchange with the utility grid, the cost of power exchange with integrated microgrids, and the cost of unserved energy in the islanded operation. The indices m, i, t, k, and s represent the microgrids, the DERs, inter-hour time periods, intra-hour time periods and the scenarios, respectively. Index n is further added for the connected microgrids. It should also be mentioned that the inter-hour time intervals and the intra-hour time intervals belong to sets {1, 2, 3,…T} and {1, 2, 3,…K}, respectively [6]. The dispatchable DGs generation cost is represented as a single-step price value c_{mi} times the amount of generation of that individual dispatchable unit $P_{mi,tks}$, which can be extended to consider multiple price steps. The cost of power exchange with the utility grid is calculated as the market price $\rho_{m,tk}$ times the amount of exchanged power $P^{M}_{m,tks}$. This term could be positive (representing cost) or negative (representing benefit) for each microgrid, based on the flow direction (i.e., power import or export). The third term represents the cost of the power exchange with the integrated microgrids, which is calculated as the local power exchange price $\lambda_{mn,tk}$ times the amount of the power exchange $P^{G}_{mn,tks}$ with integrated microgrids. This term could be either a cost or a benefit depending on the flow direction. It should be noted that this term is always zero, as every power exchange is counted twice, once with a positive sign (from microgrid m to microgrid n) and once with a negative sign (from microgrid n to microgrid m). This term is included in the objective for the purpose of decomposition that is discussed later. The last term in the objective represents the cost of the unserved energy, i.e., the cost of the load curtailment, which only occurs during the islanded mode. This term is determined as the value of lost load (VOLL) $\upsilon_{m,tk}$ times the amount of curtailed load $LS_{m,tks}$ in each microgrid m. This term is added to the objective function to account for system reliability.

The grid-connected and the islanded operation modes are differentiated in the objective function and later in the constraints, using scenario s, where $s = 0$ denotes the grid-connected mode and $s \geq 1$ denotes the islanded mode [35,47]. The objective is subject to operational constraints, as follows:

$$P^{\min}_{mi}I_{mi,t} \leq P_{mi,tks} \leq P^{\max}_{mi}I_{mi,t} \quad \forall\, m, \forall\, i, \forall\, t, \forall\, k, \forall\, s \quad (2)$$

$$\sum_{i\in A} P_{mi,tks} + P^{M}_{m,tks} + \sum_{n\in M,n\neq m} P^{G}_{mn,tks} + LS_{m,tks} = D_{m,tks} \quad \forall\, m, \forall\, t, \forall\, k, \forall\, s \quad (3)$$

$$-P^{M,\max}_{m}U_{ts} \leq P^{M}_{m,tks} \leq P^{M,\max}_{m}U_{ts} \quad \forall\, m, \forall\, t, \forall\, k, \forall\, s \quad (4)$$

$$-P^{G,\max}_{mn} \leq P^{G}_{mn,tks} \leq P^{G,\max}_{mn} \quad \forall\, m, \forall\, n, \forall\, t, \forall\, k, \forall\, s \quad (5)$$

$$P^{G}_{mn,tks} + P^{G}_{nm,tks} = 0 \quad \forall\, m, \forall\, n, \forall\, t, \forall\, k, \forall\, s \quad (6)$$

The dispatchable unit generation is subject to capacity and commitment limits, which are imposed using lower/upper generation values and the commitment state of the unit, as presented in (2). The power balance Eq. (3) ensures that the sum of power generated by local DERs, exchanged with the utility grid, and exchanged with the integrated microgrids matches the local load. The load curtailment variable is further added to the load balance equation to ensure a feasible solution during islanded operation. Microgrids' power exchange with the utility grid is limited by the flow limits of the associated connecting line, as presented in (4), which will be further imposed to zero during the islanded operation using a binary islanding indicator. Each microgrid's power exchange with integrated microgrids is limited by the limits of the associated connecting line, as presented in (5). Finally, constraint (6) denotes that the summation of the local power exchange between any two connected microgrids is zero, i.e., it ensures that the amount of power offered by microgrid m/n is entirely provided to microgrid n/m, since they are equal in value but opposite in sign. Of course the power losses in the lines connecting the integrated microgrids are assumed to be negligible due to their proximity.

It is deduced from the proposed system aggregated model that the only coupling constraint among integrated microgrids is the power exchange among microgrids, represented in (6). In other words, if this term could be eliminated, the problem could be decomposed into m individual optimal scheduling problems, each associated with one microgrid. This can be achieved by penalizing the constraint (6) and adding it to the objective function.

3.2. Individual microgrid problem

Constraint (6) is penalized in the objective function using a Lagrangian multiplier μ. Accordingly, the proposed model is decomposed to m individual problems, one for each microgrid. This is possible due to the summation over m in the objective function and the fact that constraints are defined for each microgrid without any coupling to other microgrids. The microgrid optimal scheduling problem is therefore modeled as follows:

$$\min \tau \sum_{t\in T_T}\sum_{k\in T_K}\sum_{s\in N}\psi_s\left(\sum_{i\in G} c_{mi}P_{mi,tks} + \rho_{m,tk}P^{M}_{m,tks} + \sum_{n\in M,n\neq m}(\lambda_{mn,tks} + \mu_{mn,tks})P^{G}_{mn,tks} + \upsilon_{m,tk}LS_{m,tks}\right) \quad (7)$$

$$\sum_{i\in A} P_{mi,tks} + P^{M}_{m,tks} + \sum_{n\in M,n\neq m} P^{G}_{mn,tks} + LS_{m,tks} = D_{m,tks} \quad \forall\, t, \forall\, k, \forall\, s \quad (8)$$

$$-P^{M,\max}_{m}U_{ts} \leq P^{M}_{m,tks} \leq P^{M,\max}_{m}U_{ts} \quad \forall\, t, \forall\, k, \forall\, s \quad (9)$$

$$-P^{G,\max}_{mn} \leq P^{G}_{mn,tks} \leq P^{G,\max}_{mn} \quad \forall\, n, \forall\, t, \forall\, k, \forall\, s \quad (10)$$

The objective is to minimize the operation cost (7), consisting of the local generation cost, cost of power exchange with the utility grid, cost of power exchange with integrated microgrids, and the cost of unserved energy. Constraints include the power balance Eq. (8), utility grid power exchange and islanding limit (9), and integrated microgrids power exchange (10). The microgrid optimal scheduling problem is further subject to operational constraints for each component within each microgrid m, including dispatchable generators (11)–(15), DES (16)–(22), and adjustable loads (23)–(25).

$$P^{\min}_{mi}I_{mi,t} \leq P_{mi,tks} \leq P^{\max}_{mi}I_{mi,t} \quad \forall\, i \in \mathrm{G}, \forall\, t, \forall\, k, \forall\, s \quad (11)$$

$$P_{mi,tks} - P_{mi,t(k-1)s} \leq UR_i \quad \forall\, i \in \mathrm{G}, \forall\, t, k \neq 1, \forall\, s \quad (12a)$$

$$P_{mi,t1s} - P_{mi,(t-1)Ks} \leq UR_i \quad \forall\, i \in \mathrm{G}, \forall\, t, \forall\, s \quad (12b)$$

$$P_{mi,t(k-1)s} - P_{mi,tks} \leq DR_i \quad \forall\, i \in \mathrm{G}, \forall\, t, k \neq 1, \forall\, s \quad (13a)$$

$$P_{mi,(t-1)Ks} - P_{mi,t1s} \leq DR_i \quad \forall\, i \in \mathrm{G}, \forall\, t, \forall\, s \quad (13b)$$

$$T^{\mathrm{on}}_{mi} \geq UT_{mi}(I_{mi,t} - I_{mi,(t-1)}) \quad \forall\, i \in \mathrm{G}, \forall\, t, s = 0 \quad (14)$$

$$T_{mi}^{\text{off}} \geq DT_{mi}(I_{mi,(t-1)} - I_{m,it}) \quad \forall\, i \in \text{G},\ \forall\, t,\ s = 0 \tag{15}$$

$$P_{mi,tks} \geq P_{mi,tk}^{\text{dch,min}} u_{mi,t} - P_{mi,tk}^{\text{ch,max}} v_{mi,t} \quad \forall\, i \in \text{S},\ \forall\, t, \forall\, k, \forall\, s \tag{16}$$

$$P_{mi,tks} \geq P_{mi,tk}^{\text{dch,min}} u_{mi,t} - P_{mi,tk}^{\text{ch,max}} v_{mi,t} \quad \forall\, i \in \text{S},\ \forall\, t, \forall\, k, \forall\, s \tag{17}$$

$$C_{mi,tks} = C_{mi,t(k-1)s} - P_{mi,tks} u_{mi,t} \tau/\eta_i \quad \forall\, i \in \text{S},\ \forall\, t,\ k \neq 1, \forall\, s - P_{mi,tks} v_{mi,t} \tau \tag{18a}$$

$$C_{mi,t1s} = C_{mi,(t-1)Ks} - P_{mi,t1s} u_{mi,t} \tau/\eta_i - P_{mi,t1s} v_{mi,t} \tau \quad \forall\, i \in \text{S},\ \forall\, t, \forall\, s \tag{18b}$$

$$C_{mi}^{\min} \leq C_{mi,tks} \leq C_{mi}^{\max} \quad \forall\, i \in \text{S},\ \forall\, t, \forall\, k, \forall\, s \tag{19}$$

$$T_{mi}^{\text{ch}} \geq MC_{mi}(u_{mi,t} - u_{mi,(t-1)}) \quad \forall\, i \in \text{S},\ \forall\, t,\ s = 0 \tag{20}$$

$$T_{mi}^{\text{dch}} \geq MD_{mi}(v_{mi,t} - v_{mi,(t-1)}) \quad \forall\, i \in \text{S},\ \forall\, t,\ s = 0 \tag{21}$$

$$u_{mi,ts} + v_{mi,ts} \leq 1 \quad \forall\, i \in \text{S},\ \forall\, t,\ s = 0 \tag{22}$$

$$D_{md,tk}^{\min} z_{md,t} \leq D_{md,tks} \leq D_{md,tk}^{\max} z_{md,t} \quad \forall\, d \in \text{D}_\text{A},\ \forall\, t, \forall\, k, \forall\, s \tag{23}$$

$$\sum_{[\alpha_d,\beta_d]} D_{md,tks} = E_{md} \quad \forall\, d \in \text{D}_\text{A}\ ,\forall\, s \tag{24}$$

$$T_{md}^{\text{on}} \geq MU_{md}(z_{md,t} - z_{md,(t-1)}) \quad \forall\, d \in \text{D}_\text{A},\ \forall\, t,\ s = 0 \tag{25}$$

The generation of the dispatchable DGs in each microgrid m is constrained by maximum and minimum generation capacity limits (11), and further multiplied by a binary variable to indicate the commitment state of that individual DG. Ramping up and down for each DG are satisfied by (12) and (13), respectively. Eqs. (12a) and (13a) represent the ramping constraints for intra-hour intervals, while (12b) and (13b) represent the ramping constraints for inter-hour time intervals. Each dispatchable DG is subject to a minimum ON time once it is switched on, which is constrained in (14), and further subject to a minimum OFF time once it is shut down, which is satisfied by (15). Constraints (16)–(22) are provided to optimally manage the operation of the DES. The DES is subject to maximum and minimum charging and discharging limits, which are constrained by (16)–(17), and further multiplied by binary variables $u_{mi,t}$ and $v_{mi,t}$ to indicate its operation status, i.e., either charging or discharging. The stored energy in the DES is calculated in (18a) and (18b), respectively, for intra-hour and inter-hour time intervals, based on the available stored energy, amount of charged and discharged energy, and DES efficiency. The time period of charging and discharging is considered to be $\tau = (1/\text{K})\text{h}$, where K is the number of intra-hour periods and h represents a time period of one hour. The stored energy in the DES is limited by the DES capacity as in (19). The DES is subject to minimum successive operating time limits for both charging and discharging, which are constrained by (20)–(21), respectively. Constraint (22) is provided to guarantee one operating mode at the scheduling time, i.e., either charging or discharging. Finally, (23)–(25) are provided to manage the operation of the installed adjustable loads in each microgrid m. Adjustable loads are restricted by maximum and minimum rated power limits, which are constrained by (23). The total required energy to accomplish the operating cycle for certain adjustable loads is satisfied by (24). In addition, some adjustable loads are subject to minimum successive operating time once they are switched on, which is satisfied by (25). It should be noted that hourly commitment is still considered for DERs in the proposed model. However, the proposed model is generic and a higher resolutions could be considered for DERs' commitment without loss of generality.

3.3. Coordination through price signal update

The proposed optimal microgrids scheduling problem can be solved by the master controller of each microgrid. The coordination among integrated microgrids is carried out via price updates.

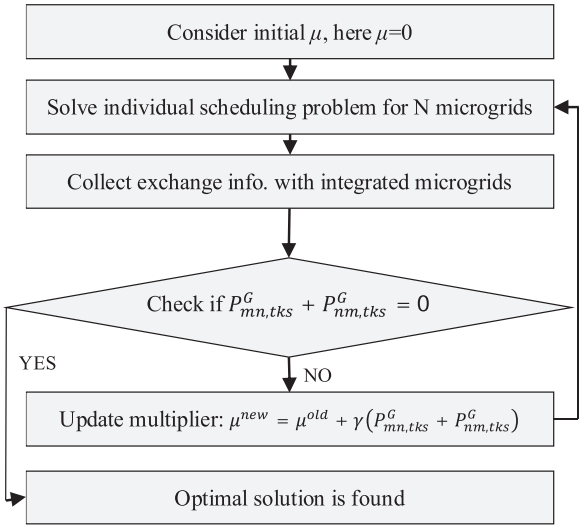

Fig. 2. Flowchart of proposed iteration procedure.

Based on the obtained objective, the price of purchasing power from microgrid n is $\lambda_{mn} + \mu_{mn}$, where λ_{mn} is a constant original price and μ_{mn} is the added Lagrangian multiplier. The same price is used for microgrid n that sells energy to microgrid m. To control the power exchange between two microgrids, the Lagrangian multiplier between these two needs to be controlled. Fig. 2 depicts the flowchart of the coordination among integrated microgrids. Initially the Lagrangian multiplier is assumed to be zero to solve the microgrid optimal scheduling problem. After obtaining all the scheduling solutions, the penalized constraint (26) is checked to examine if the solution is feasible. If not, the Lagrangian multiplier is updated using (27), where γ is a constant positive number.

$$P^G_{mn,tks} + P^G_{nm,tks} = 0 \quad \forall\, m, \forall\, n,\ \forall\, t, \forall\, k, \forall\, s \tag{26}$$

$$\mu^{new} = \mu^{old} + \gamma(P^G_{mn,tks} + P^G_{nm,tks}) \quad \forall\, m, \forall\, n,\ \forall\, t, \forall\, k, \forall\, s \tag{27}$$

Based on (27), if the summation $P^G_{mn,tks} + P^G_{nm,tks}$ is positive, the exchange needs to be reduced, which will be done by increasing μ and making the power exchange with integrated microgrids less attractive (a larger μ in the objective results in a smaller $P^G_{mn,tks}$). Similarly, if the summation $P^G_{mn,tks} + P^G_{nm,tks}$ is negative, the exchange needs to be increased by decreasing μ, hence making the power exchange with integrated microgrids more attractive. The iterative price update and scheduling process will continue until it converges, i.e., (26) is satisfied for all microgrids and connections.

4. Numerical simulations

An integrated microgrid test system with two microgrids is utilized to evaluate the performance and effectiveness of the proposed model. Microgrid A comprises four dispatchable units, two nondispatchable units, and one DES with 95% efficiency. Microgrid B comprises five dispatchable units, two nondispatchable units, and five adjustable loads. Microgrids characteristics (including loads consumption) are summarized in Tables 1 and 2. Hourly forecasted market prices, borrowed from Ref. [7], are listed in Table 3. The power exchange with the utility grid is limited by the connecting line capacity limit, which is assumed for both microgrids to be 10 MW. The local power exchange among the integrated microgrids is further subject to a line capacity limit of 4 MW. It is worth mentioning that six intra-hour time intervals, i.e., K equal to 6, are considered in simulations. In other words, a ten-minute resolution in a 24-h scheduling horizon is considered in this section. A total of 145 scenarios are considered in this study, where

Table 1
Microgrid A characteristics.

Dispatchable units

Unit	Cost coefficient ($/MWh)	Min.–max. capacity (MW)	Min. up/down time (h)	Ramp up/down rate (MW/h)
G1	27.7	1–5	3	2.5
G2	39.1	1–5	3	2.5
G3	61.3	0.8–3	1	3
G4	65.6	0.8–3	1	3

Aggregated generation of nondispatchable units

Time (h)	1	2	3	4	5	6	7	8
Power (MW)	0	0	0	0	0.63	0.80	0.62	0.71
Time (h)	9	10	11	12	13	14	15	16
Power (MW)	0.68	0.35	0.62	1.11	1.21	1.57	1.23	1.28
Time (h)	17	18	19	20	21	22	23	24
Power (MW)	1.05	0.82	0.71	0.92	0.57	0.60	0	0

DES

Storage	Capacity (MWh)	Min.–max. charging/discharging power (MW)	Min. charging/discharging time (h)
DES1	10	0.4–2	5

Hourly fixed load

Time (h)	1	2	3	4	5	6	7	8
Load (MW)	9.00	8.80	8.73	9.31	9.06	9.08	10.43	11.27
Time (h)	9	10	11	12	13	14	15	16
Load (MW)	11.54	12.14	12.45	12.50	14.35	15.74	15.83	16.18
Time (h)	17	18	19	20	21	22	23	24
Load (MW)	16.63	16.64	16.04	15.99	14.43	13.43	10.12	9.74

scenario 0 denotes the grid-connected operation and scenarios 1–144 represent the islanded operation. Each islanding scenario denotes the islanding operation in a specific ten-minute time interval, i.e., a T-1 islanding criterion. The problem is modeled and solved using CPLEX 11.0 [53]. Five cases are examined to investigate the power exchange merits among the integrated microgrids.

Case 1: independent scheduling: In this case each of the microgrids are autonomously scheduled (no power exchange) during both operation modes, i.e., in the grid-connected and islanded modes. As shown in Table 9, the total operation costs for microgrids A and B are $8908 and $21,570, respectively. Fig. 3 depicts the exchanged power of Microgrid A and Microgrid B with the utility grid during the grid-connected mode. It is observed from Fig. 3 and Table 3 that, both microgrids import power in low price hours and export or decrease their import in high price hours to minimize their operation costs. In the islanded mode, the optimal scheduling of the installed DES in Microgrid A supports avoiding the undesired load shedding in this microgrid; the average load curtailment in Microgrid B equals to 1.01 MWh, ranging from 0.66 MW to 5.17 MW in peak load hours (between hours 13 and 20). The total daily load curtailment in Microgrid B is 24.27 MWh, and Fig. 4 illustrates the hourly load curtailment in Microgrid B during the islanded operation.

Case 2: integrated scheduling: In this case the power is exchanged among the integrated microgrids during the islanded operation. The total operation cost of microgrid A is calculated as $6743.80, which implies a reduction of 24.25% compared to Case 1, due to selling power to Microgrid B and leveraging the unused capacity. On the other hand, although the total operation cost of Microgrid B is increased to $23,543.93, its average load curtailment is reduced to 0.29 MWh, i.e., a reduction of 70.87% compared to Case 1, which implies significant improvement of reliability. Table 9 summarizes the total operation costs of two microgrids and total curtailed loads in Microgrid B, for

Table 2
Microgrid B characteristics.

Dispatchable units

Unit	Cost coefficient ($/MWh)	Min.–max. capacity (MW)	Min. up/down time (h)	Ramp up/down rate (MW/h)
G1	26.8	1–6	3	3
G2	35.5	1–6	3	3
G3	64.1	0.8–3	1	3
G4	72.3	0.8–3	1	3
G5	85.6	1–3	1	3

Aggregated generation of nondispatchable units

Time (h)	1	2	3	4	5	6	7	8
Power (MW)	0	0	0	0	0.71	0.92	0.79	0.83
Time (h)	9	10	11	12	13	14	15	16
Power (MW)	0.79	0.47	0.74	1.31	1.47	1.69	1.31	1.36
Time (h)	17	18	19	20	21	22	23	24
Power (MW)	1.23	1.02	0.89	1.13	0.63	0.72	0	0

Adjustable loads (S: shiftable, C: curtailable)

Load	Type	Min.–max. capacity (MW)	Required energy (MWh)	Required start–end time (h)	Min. up time (h)
L1	S	0–0.4	1.6	11–15	1
L2	S	0–0.4	1.6	15–19	1
L3	S	0.02–0.8	2.4	16–18	1
L4	S	0.02–0.8	2.4	14–22	1
L5	C	1.8–2	47	1–24	24

Hourly fixed load

Time (h)	1	2	3	4	5	6	7	8
Load (MW)	17.05	16.60	15.62	17.35	18.07	19.12	18.51	17.31
Time (h)	9	10	11	12	13	14	15	16
Load (MW)	16.49	18.16	18.43	20.46	21.33	22.69	23.91	24.21
Time (h)	17	18	19	20	21	22	23	24
Load (MW)	24.76	24.59	22.11	21.93	19.62	17.39	17.09	16.69

both cases. Fig. 4 compares the hourly load curtailment in Microgrid B during the islanded operation in Cases 1 and 2. As Fig. 4 depicts, the load curtailment of Microgrid B in Case 2, allowing interaction between microgrids, is reduced to three hours in a day, compared to eight hours in Case 1. Moreover, this reliability improvement represents a saving of $172,000 in terms of outages (assuming a relatively small VOLL of $10/kWh [54]). Commitment states of the dispatchable units and the DES for both microgrids in Case 2 are listed in Tables 4 and 5, respectively, where bold values imply changes from Case 1. It is observed that the commitment status of the DES in Microgrid A and G5 in Microgrid B are changed from Case 1 to Case 2, to achieve the least-cost reliability-constrained schedule for both microgrids.

The hourly power exchange between the two microgrids is shown in Table 6. As the table shows, the hourly exchanged power among the integrated microgrids varies between 0.4 MW and 3.4 MW, based on the available capacity in the microgrids while taking into account the supply-demand balance for the entire system.

Fig. 5 shows the exchanged power of both microgrids with the utility grid during the grid-connected mode Case 2. It is observed that the exchanged power in Case 2 is almost the same as Case 1, with slight changes in three hours. These insignificant changes are due to revised schedules of DES and DGs. The two microgrids are connected to the same bus, accordingly same price, at the utility side in grid-connected mode. It should be noted that the exchanged power between microgrids is zero during the grid-connected mode, as the optimal scheduling enforces them to exchange power with the utility grid instead of with the other microgrid. To clarify this issue, assume that there is adequate line capacity between each microgrid and the utility grid, Microgrid A has

Table 3
Hourly market price.

Time (h)	1	2	3	4	5	6	7	8
Price ($/MWh)	15.03	10.97	13.51	15.36	18.51	21.80	17.30	22.83
Time (h)	9	10	11	12	13	14	15	16
Price ($/MWh)	21.84	27.09	37.06	68.95	65.79	66.57	65.44	79.79
Time (h)	17	18	19	20	21	22	23	24
Price ($/MWh)	115.45	110.28	96.05	90.53	77.38	70.95	59.42	56.68

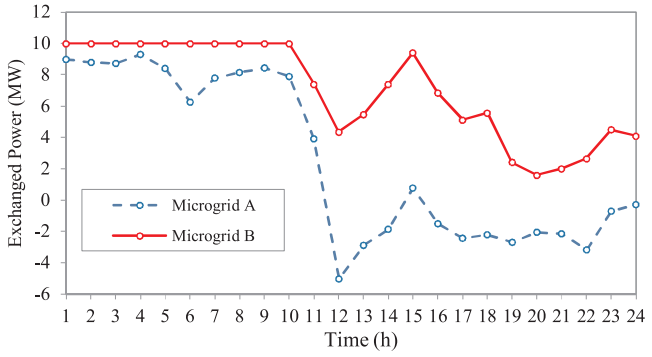

Fig. 3. Power exchange with the utility grid during the grid-connected mode in Case 1.

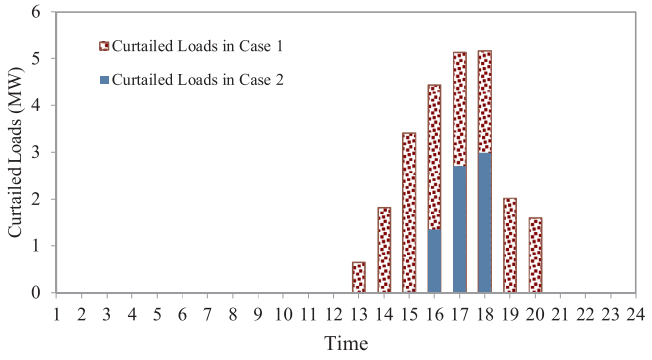

Fig. 4. Microgrid B load curtailment during the islanded operation.

surplus generation, and Microgrid B has deficiet power. In case the utility price is higher than the local power exchange price, Microgrid B would be interested in purchasing power form Microgrid A; however, Microgrid A would sell its surplus generation to the utility grid as it would result in higher profit. The same is true when the utility price is lower than the local power exchange price; where Microgrid B in this case prefers to import its power need from the utility grid rather than Microgrid A, as it is cheaper and would further minimizes its operation cost.

Fig. 6 shows the sensitivity of load curtailment in Microgrid B and total operation cost of both microgrids with respect to the maximum line capacity between microgrids. Results show that the Microgrid A operation cost decreases by increasing the line capacity limit, while the Microgrid B operation cost increases by increasing the line capacity limit. The increase in Microgrid B operation cost is due to the increased power import from Microgrid A to alleviate the load curtailment (which is decreased by increasing the limit of the line) and to enhance the local reliability.

Case 3: both microgrids have deficient generation: In this case, the fixed load in Microgrid A is increased by 35% to investigate its impact on the power exchange scheduling among the integrated microgrids when both microgrids have deficient generation. In this case, the power is exchanged among the integrated microgrids in only two hours (i.e., 8 and 21). The exported power from Microgrid A to Microgrid B in hour 8 is 0.28 MW, while the exported power from Microgrid B to Microgrid A in hour 21 is 0.19 MW, which are illustrated in Table 7. Power exchange between the microgrids, while both have deficient generation, minimizes the individual operation cost along with the system aggregated operation cost. Nevertheless, in this case, both microgrids encounter load curtailments, which are shown in Fig. 7. Microgrid A's operation cost increases to $15,642.58, increased

Table 4
Dispatchable units and DES schedule for Microgrid A.

Hour (1–24)																								
G1	1	1	1	1	1	1	1	1	1	1	1	1	1	1	1	1	1	1	1	1	1	1	1	1
G2	1	1	1	1	1	1	1	1	1	1	1	1	1	1	1	1	1	1	1	1	1	1	1	1
G3	0	0	0	0	0	0	0	0	0	0	0	1	1	1	1	1	1	1	1	1	1	1	1	0
G4	0	0	0	0	0	0	0	0	0	0	0	1	1	1	1	1	1	1	1	1	1	1	0	0
DES	−1	−1	−1	−1	−1	0	0	1	1	1	1	1	0	0	**1**	1	1	1	1	1	0	0	0	0

Bold values imply changes from Case 1 to Case 2.

Table 5
Dispatchable units schedule for Microgrid B.

Hour (1–24)																								
G1	1	1	1	1	1	1	1	1	1	1	1	1	1	1	1	1	1	1	1	1	1	1	1	1
G2	1	1	1	1	1	1	1	1	1	1	1	1	1	1	1	1	1	1	1	1	1	1	1	1
G3	1	1	1	1	1	1	1	1	1	1	1	1	1	1	1	1	1	1	1	1	1	1	1	1
G4	1	1	1	1	1	1	1	1	1	1	1	1	1	1	1	1	1	1	1	1	1	1	1	1
G5	1	**0**	0	1	**0**	1	1	**0**	0	1	1	1	1	1	1	1	1	1	1	1	1	1	**0**	1

Bold values imply changes from Case 1 to Case 2.

Table 6
Power exchange among integrated microgrids.

Time (h)	1	2	3	4	5	6	7	8
P^{A-B} (MW)	0	−0.4	0	0	−1.16	0	0	−0.28
P^{B-A} (MW)	0	0.4	0	0	1.16	0	0	0.28
Time (h)	9	10	11	12	13	14	15	16
P^{A-B} (MW)	0	0	0	0	−0.66	−1.82	−3.4	−3.1
P^{B-A} (MW)	0	0	0	0	0.66	1.82	3.4	3.1
Time (h)	17	18	19	20	21	22	23	24
P^{A-B} (MW)	−2.42	−2.18	−2.02	−1.6	0	0	−0.89	0
P^{B-A} (MW)	2.42	2.18	2.02	1.6	0	0	0.89	0

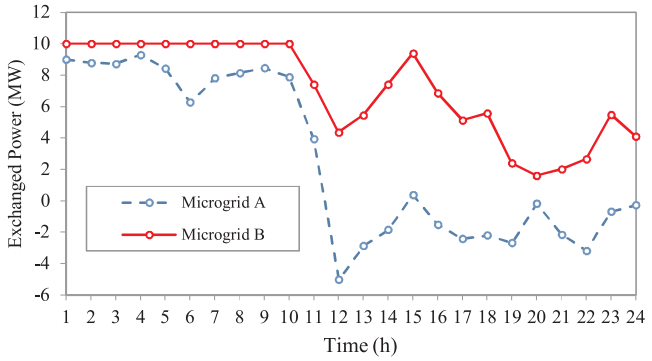

Fig. 5. Power exchange with the utility grid during the grid-connected mode in Case 2.

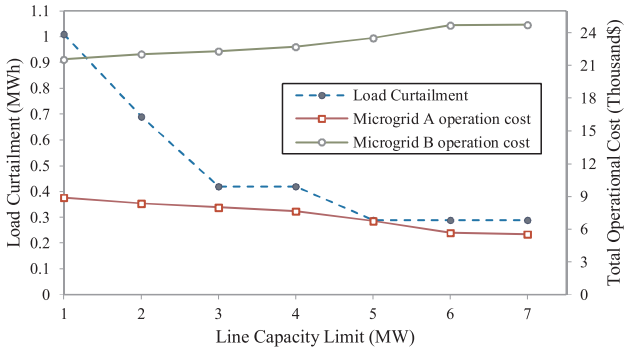

Fig. 6. Sensitivity analysis of load curtailment and microgrid operation cost with respect to line capacity limit.

Table 7
Power exchange among integrated microgrids in Case 3.

Time (h)	1	2	3	4	5	6	7	8
P^{A-B} (MW)	0	0	0	0	0	0	0	−0.28
P^{B-A} (MW)	0	0	0	0	0	0	0	0.28
Time (h)	9	10	11	12	13	14	15	16
P^{A-B} (MW)	0	0	0	0	0	0	0	0
P^{B-A} (MW)	0	0	0	0	0	0	0	0
Time (h)	17	18	19	20	21	22	23	24
P^{A-B} (MW)	0	0	0	0	0.19	0	0	0
P^{B-A} (MW)	0	0	0	0	−0.19	0	0	0

by 75.7% compared with the base case, due to the increase in the local demand. On the other side, even though Microgrid B encounters load curtailment equals to the base case, it saves $86.5 in terms of the operation cost compared to the base case. Table 9 shows the integrated microgrids operation cost. This study indicates that the power exchange scheduling among the integrated microgrids relies on the unused capacity in each microgrid in the integrated system, and further on the

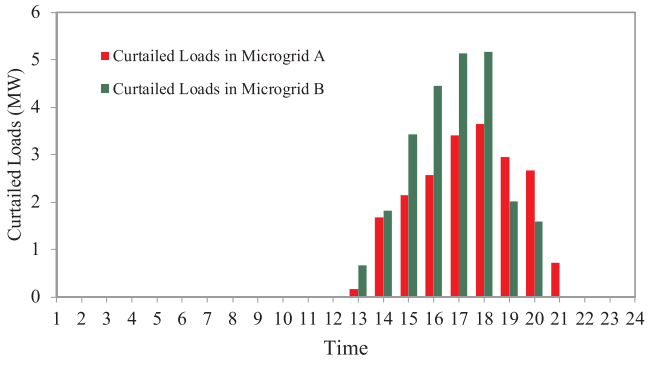

Fig. 7. Microgrids load curtailments during the islanded operation in Case 3.

Table 8
Power exchange among integrated microgrids in Case 4.

Time (h)	1	2	3	4	5	6	7	8
P^{A-B} (MW)	0	−0.59	0	0	−0.835	−1.308	0	0
P^{B-A} (MW)	0	0.59	0	0	0.835	1.308	0	0
Time (h)	9	10	11	12	13	14	15	16
P^{A-B} (MW)	0	0	0	0	0	0	−1.051	0
P^{B-A} (MW)	0	0	0	0	0	0	1.051	0
Time (h)	17	18	19	20	21	22	23	24
P^{A-B} (MW)	0	0	0	0	0	0	0	0
P^{B-A} (MW)	0	0	0	0	0	0	0	0

Table 9
Total operation cost and curtailed load.

Case no.	Microgrid A operation cost	Microgrid B operation cost	System total operation cost	Curtailed load in Microgrid A	Curtailed load in Microgrid B
Case 1	$8903.04	$21,570.62	$30,473.66	–	24.27 MWh
Case 2	$6743.80	$23,543.93	$30,287.73	–	7.07 MWh
Case 3	$15,642.58	$21,484.12	$37,126.7	19.92 MWh	24.27 MWh
Case 4	$8894.68	$10,663.02	$19,557.7	–	–
Case 5	$6740.15	$23,533.92	$30,274.07	–	7.03 MWh

generation cost of the dispatchable DGs in all microgrids to minimize the individual operation cost and the aggregated system operation cost.

Case 4: both microgrids have surplus generation: In this case, the fixed load in Microgrid B is decreased by 35% to investigate its impact on the power exchange scheduling among the integrated microgrids when both microgrids have surplus generation. Even though both microgrids have surplus generation, the power is exchanged among the integrated microgrids in four hours (i.e., 2, 5, 6, and 15), which are illustrated in Table 8, in order to minimize the entire system operation cost. Microgrid A's operation cost is $8894.68, while Microgrid B's operation cost is $10,663.02, which are shown in Table 9. The load curtailments in this case for both microgrids are zero due to the surplus in the generation.

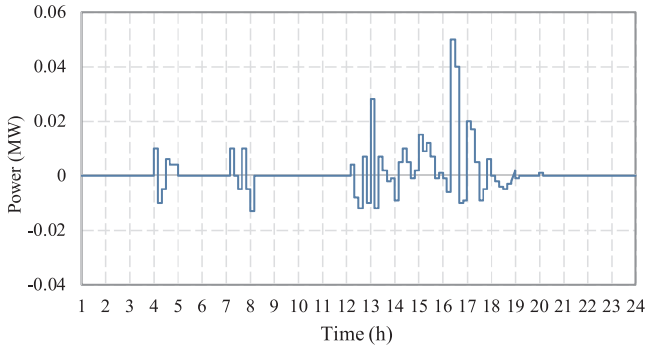

Fig. 8. The difference of the power exchange among the integrated microgrids between the high resolution and the low resolution cases.

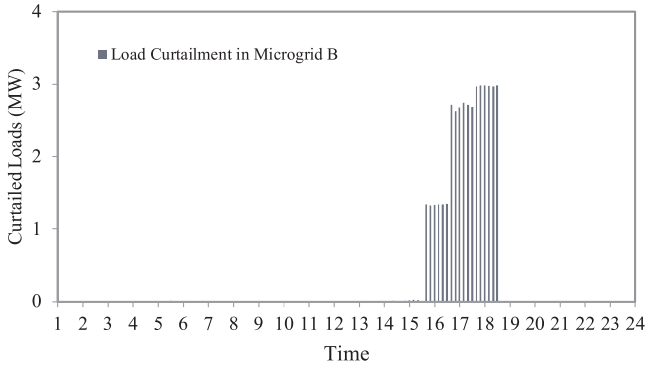

Fig. 9. Microgrid B load curtailment with a higher resolution.

The obtained results show that all decisions are based on the microgrids operation cost, not on the surplus or deficit in generation. However, it should be noted that the proposed optimal scheduling model motivates the power exchange between the integrated microgrids, when one of the microgrids can offer power with a lower cost compared to the generation cost of the already installed DERs at the other microgrid. This would positively impact the economic benefits for both microgrids. In other words, the proposed optimal scheduling model is generic and could be applied to integrated microgrids under any operational settings.

Case 5: high resolution: In this case, the optimal scheduling problems for Case 2 is solved again but with considering 10 min intra-hour time periods (sub-hourly) to investigate the high resolution capability of the proposed model. The differences in the power exchange scheduling of the integrated microgrids in this case compared with the lower resolution in Case 2 is depicted in Fig. 8. Slight differences can be seen between the two cases, which is due to the capability to capture the variability and volatility of loads and renewable generations in Case 5. Total curtailed load in Microgrid B, in this case, is 7.03 MWh, which is reduced by 0.57% compared with Case 2 as illustrated in Fig. 9. It is seen that the load curtailment in this case is almost similar to Case 2, however with a higher resolution. The integrated microgrids operation cost considering the high resolution are shown in Table 9, where the system aggregated operation cost is reduced by 0.045% compared with Case 2.

It should be noted that the microgrids privacy is highly protected while performing these numerical simulations and the only information that is exchanged is the local power exchange prices signals, iteratively. Furthermore, it is worth to mention that the proposed model is generic and could be employed with smaller intra-hour time periods to capture the rapid changes in loads and renewable generations.

5. Discussions and conclusion

Microgrids can be utilized in an integrated fashion in order to leverage their available/unused capacity for supporting other connected microgrids that lack adequate power. This paper developed an optimal scheduling model of integrated microgrids, which utilized the LR method to find an optimal solution while minimizing data sharing among microgrids. The presented LR model determined the least-cost schedule of all microgrids' loads and DERs and provided the optimal scheduling for all integrated microgrids. Moreover, the proposed model could ensure that the amount of load shedding for all integrated microgrids is minimized, thereby increasing the system reliability. In addition, the privacy concerns were taken into account in the proposed optimal scheduling model of integrated microgrids, while ensuring that all microgrids could reach their associated least-cost schedule without sharing any private data with other microgrids. A high resolution optimal scheduling for the integrated microgrids systems was further presented, taking into account intra-hour and inter-hour time periods, to capture the variability and volatility of the renewable generation and loads. Numerical simulations on a test system showed a reduction in the total operation cost and improvement in system reliability of integrated microgrids based on the proposed model, advocating on its acceptable performance and practical merits.

References

[1] M. Shahidehpour, J. Clair, A functional microgrid for enhancing reliability, sustainability, and energy efficiency, Electr. J. 25 (October (8)) (2012) 21–28.
[2] A. Khodaei, M. Shahidehpour, Microgrid-based co-optimization of generation and transmission planning in power systems, IEEE Trans. Power Syst. 28 (May (2)) (2013) 1582–1590.
[3] N. Hatziargyriou, H. Asano, M.R. Iravani, C. Marnay, Microgrids: an overview of ongoing research, development and demonstration projects, IEEE Power Energy Mag. 5 (July/August (4)) (2007) 78–94.
[4] P.M. Costa, M.A. Matos, Assessing the contribution of microgrids to the reliability of distribution networks, Electr. Power Syst. Res. 79 (February (2)) (2009) 382–389.
[5] A. Khodaei, Resiliency-oriented microgrid optimal scheduling, IEEE Trans. Smart Grid 5 (July (4)) (2014) 1584–1591.
[6] A. Majzoobi, A. Khodaei, Application of microgrids in supporting distribution grid flexibility, IEEE Trans. Power Syst. 32 (September (5)) (2017) 3660–3669.
[7] A. Khodaei, Microgrid optimal scheduling with multi-period islanding constraints, IEEE Trans. Power Syst. 29 (May (3)) (2014) 1383–1392.
[8] K. Balasubramaniam, P. Saraf, R. Hadidi, E.B. Makram, Energy management system for enhanced resiliency of microgrids during islanded operation, Electr. Power Syst. Res. 137 (August) (2016) 133–141.
[9] W. Saad, Z. Han, H.V. Poor, Coalitional game theory for cooperative micro-grid distribution networks, Proc. IEEE International Conference on Communication Workshops (ICC), Kyoto, Japan, June, 2011, pp. 1–5.
[10] G.S. Kasbekar, S. Sarkar, Pricing games among interconnected microgrids, Proc. IEEE PES General Meeting, July, 2012, pp. 1–8.
[11] D.I. Papaioannou, C.N. Papadimitriou, A.L. Dimeas, E.I. Zountouridou, G.C. Kiokes, N.D. Hatziargyriou, Optimization & sensitivity analysis of microgrids using HOMER software—a case study, MedPower, Athens, 2014, pp. 1–7.
[12] H. Dagdougui, L. Dessaint, A. Ouammi, Optimal power exchanges in an interconnected power microgrids based on model predictive control, IEEE PES General Meeting Conference & Exposition, National Harbor, MD, July, 2014.
[13] K. Rahbar, C.C. Chai, R. Zhang, Real-time energy management for cooperative microgrids with renewable energy integration, IEEE International Conference on Smart Grid Communications (SmartGridComm), Venice, Italy, November, 2014.
[14] Y. Li, N. Liu, J. Zhang, Jointly optimization and distributed control for interconnected operation of autonomous microgrids, IEEE Innovative Smart Grid Technologies—Asia (ISGT ASIA), Bangkok, Thailand, November, 2015.
[15] Y. Li, N. Liu, C. Wu, J. Zhang, Distributed optimization of generation scheduling of interconnected microgrids, IEEE PES Asia-Pacific Power and Energy Engineering Conference (APPEEC), Brisbane, QLD, Australia, November, 2015.
[16] F. Xiao, Q. Ai, New modeling framework considering economy, uncertainty, and security for estimating the dynamic interchange capability of multi-microgrids, Electr. Power Syst. Res. 152 (November) (2017) 237–248.
[17] M.E. Gamez Urias, E.N. Sanchez, L.J. Ricalde, Electrical microgrid optimization via a new recurrent neural network, IEEE Syst. J. 9 (September (3)) (2015).
[18] Z. Wang, B. Chen, J. Wang, C. Chen, Networked microgrids for self-healing power systems, IEEE Trans. Smart Grid 7 (January (1)) (2016).
[19] Z. Wang, B. Chen, J. Wang, M. Begovic, C. Chen, Coordinated energy management of networked microgrids in distribution systems, IEEE Trans. Smart Grid 6 (January (1)) (2015) 45–53.
[20] G.N. Korres, N.D. Hatziargyriou, P.J. Katsikas, State estimation in multi-microgrids, Int. Trans. Electr. Energy Syst. 21 (March (2)) (2011) 1178–1199.
[21] A.G. Madureira, J.C. Pereira, N.J. Gil, J.A.P. Lopes, G.N. Korres, N.D. Hatziargyriou,

Advanced control and management functionalities for multi-microgrids, Int. Trans. Electr. Energy Syst. 21 (March (2)) (2011) 1159–1177.
[22] J. Vasiljevska, J.A.P. Lopes, M.A. Matos, Evaluating the impacts of the multi-microgrid concept using multicriteria decision aid, Electr. Power Syst. Res. 91 (2012) 44–51.
[23] J. Vasiljevska, J.A.P. Lopes, M.A. Matos, Integrated micro-generation, load and energy storage control functionality under the multi micro-grid concept, Electr. Power Syst. Res. 95 (2013) 292–301.
[24] S. Moayedi, A. Davoudi, Distributed tertiary control of DC microgrid clusters, IEEE Trans. Power Electron. 31 (April (2)) (2015).
[25] A.A. Mohamed, A.T. Elsayed, T.A. Youssef, O.A. Mohammed, Hierarchical control for DC microgrid clusters with high penetration of distributed energy resources, Electr. Power Syst. Res. 148 (July) (2017) 210–219.
[26] S.A. Arefifar, Y.A.I. Mohamed, Optimized multiple microgrid-based clustering of active distribution systems considering communication and control requirements, IEEE Trans. Ind. Electron. 62 (August (2)) (2014).
[27] M. He, M. Giesselmann, Reliability-constrained self-organization and energy management towards a resilient microgrid cluster, IEEE PES Innovative Smart Grid Technologies Conference (ISGT), Washington DC, February, 2015.
[28] Q. Shafiee, T. Dragicevic, F. Andrade, J.C. Vasquez, J.M. Guerrero, Distributed consensus-based control of multiple dc-microgrids clusters, IEEE PES Innovative Smart Grid Technologies Conference (ISGT) (2015).
[29] R.H. Lasseter, Smart distribution: coupled microgrids, Proc. IEEE 99 (June (6)) (2011) 1074–1082.
[30] Q. Shafiee, T. Dragicevic, J. Vasquez, J.M. Guerrero, Modeling, stability analysis and active stabilization of multiple DC-microgrid clusters, IEEE International Energy Conference (ENERGYCON), Cavtat, Croatia, May, 2014.
[31] H. Lin, C. Liu, J.M. Guerrero, J.C. Vasquez, T. Dragicevic, Modular power architectures for microgrid clusters, International Conference on Green Energy, Sfax, Tunisia, March, 2014.
[32] L. Che, X. Zhang, M. Shahidehpour, A. Alabdulwahab, A. Abusorrah, Optimal interconnection planning of community microgrids with renewable energy sources, IEEE Trans. Smart Grid 8 (May (3)) (2017).
[33] A. Khodaei, Provisional microgrids, IEEE Trans. Smart Grid 6 (May (3)) (2015).
[34] A. Khodaei, Provisional microgrid planning, IEEE Trans. Smart Grid 8 (August (3)) (2015).
[35] A. Albaker, A. Khodaei, Elevating prosumers to provisional microgrids, Proc. IEEE PES General Meeting, Chicago, IL, USA, 2017.
[36] A. Kargarian, B. Falahati, Y. Fu, M. Baradar, Multiobjective optimal power flow algorithm to enhance multi-microgrids performance incorporating IPFC, Proc. IEEE PES General Meeting, San Diego, CA, July, 2012, pp. 1–6.
[37] Z. Wang, B. Chen, J. Wang, J. Kim, Decentralized energy management system for networked microgrids in grid-connected and islanded modes, IEEE Trans. Smart Grid 7 (June (2)) (2015) 1097–1105.
[38] A.G. Anastasiadis, A.G. Tsikalakis, N.D. Hatziargyriou, Operational and environmental benefits due to significant penetration of microgrids and topology sensitivity, Proc. IEEE PES General Meeting, Providence, RI, July, 2010.
[39] P. Li, X. Guan, J. Wu, D. Wang, An integrated energy exchange scheduling and pricing strategy for multi-microgrid system, IEEE Region 10 Conference (31194) TENCON, Xi'an, China, October, 2013, pp. 1–5.
[40] H. Wang, J. Huang, Incentivizing energy trading for interconnected microgrids, IEEE Trans. Smart Grid (in press) http://doi.org/10.1109/TSG.2016.2614988.
[41] M. Asaduz-Zaman, A.H. Chowdhury, Optimum economic dispatch of interconnected microgrid with energy storage system, Int. Conf. Electrical Engineering and Information Communication Technology (ICEEICT), Dhaka, Bangladesh, May, 2015, pp. 1–6.
[42] J. Lee, J. Guo, J.K. Choi, M. Zukerman, Distributed energy trading in microgrids: a game-theoretic model and its equilibrium analysis, IEEE Trans. Ind. Electron. 62 (June (6)) (2015) 3524–3533.
[43] N. Nikmehr, S.N. Ravadanegh, Optimal power dispatch of multi-microgrids at future smart distribution grids, IEEE Trans. Smart Grid 6 (July (4)) (2015) 1648–1657.
[44] D.T. Nguyen, L.B. Le, Optimal energy management for cooperative microgrids with renewable energy resources, IEEE International Conference on Smart Grid Communications (SmartGridComm), Vancouver, BC, Canada, 2013, pp. 678–683.
[45] A.K. Marvasti, Y. Fu, S. DorMohammadi, M. Rais-Rohani, Optimal operation of active distribution grids: a system of systems framework, IEEE Trans. Smart Grid 5 (May (3)) (2014) 1228–1237.
[46] H. Wang, J. Huang, Bargaining-based energy trading market for interconnected microgrids, IEEE International Conference on Communications (ICC), London, UK, June, 2015, pp. 776–781.
[47] A. Albaker, A. Khodaei, Communicative scheduling of integrated microgrids, Proc. IEEE Power Energy Soc. T&D, Denver, CO, April, 2018.
[48] F. Zhuang, F.D. Galiana, Towards a more rigorous and practical unit commitment by Lagrangian relaxation, IEEE Trans. Power Syst. 3 (May (2)) (1988) 763–773.
[49] T. Li, M. Shahidehpour, Price-based unit commitment: a case of Lagrangian relaxation versus mixed integer programming, IEEE Trans. Power Syst. 20 (November (4)) (2005) 2015–2025.
[50] L. Lai, L. Xie, Q. Xia, H. Zhong, C. Kang, Decentralized multi-area economic dispatch via dynamic multiplier-based Lagrangian relaxation, IEEE Trans. Power Syst. 30 (November (6)) (2015) 3225–3233.
[51] C.P. Cheng, C.W. Liu, C.C. Liu, Unit commitment by Lagrangian relaxation and genetic algorithms, IEEE Trans. Power Syst. 15 (May (2)) (2000) 707–714.
[52] A. Majzoobi, A. Khodaei, Application of microgrids in providing ancillary services to the utility grid, Energy 123 (March) (2017) 555–563.
[53] ILOG CPLEX, ILOG CPLEX Homepage [Online], 2009. Available: http://www.ilog.com.
[54] Estimating the Value of Lost Load [Online]. Available: http://www.ercot.com/content/gridinfo/resource/2015/mktanalysis/ERCOT_ValueofLostLoad_LiteratureReviewandMacroeconomic.pdf.